# Week 12

## Light Detectors 2

Measuring solar cell efficiency

OPV Architectures, Morphologies and Materials

Transparency

Chapter 7.3.3-7.4.3

# Understanding Solar Cell Efficiency Limits

Consider the Source

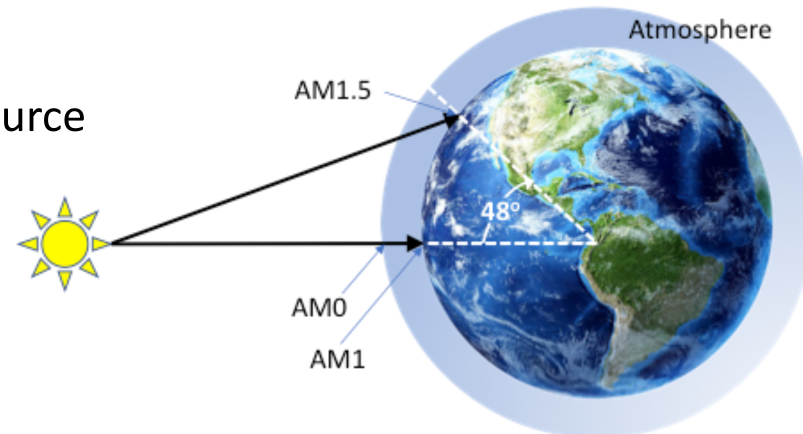


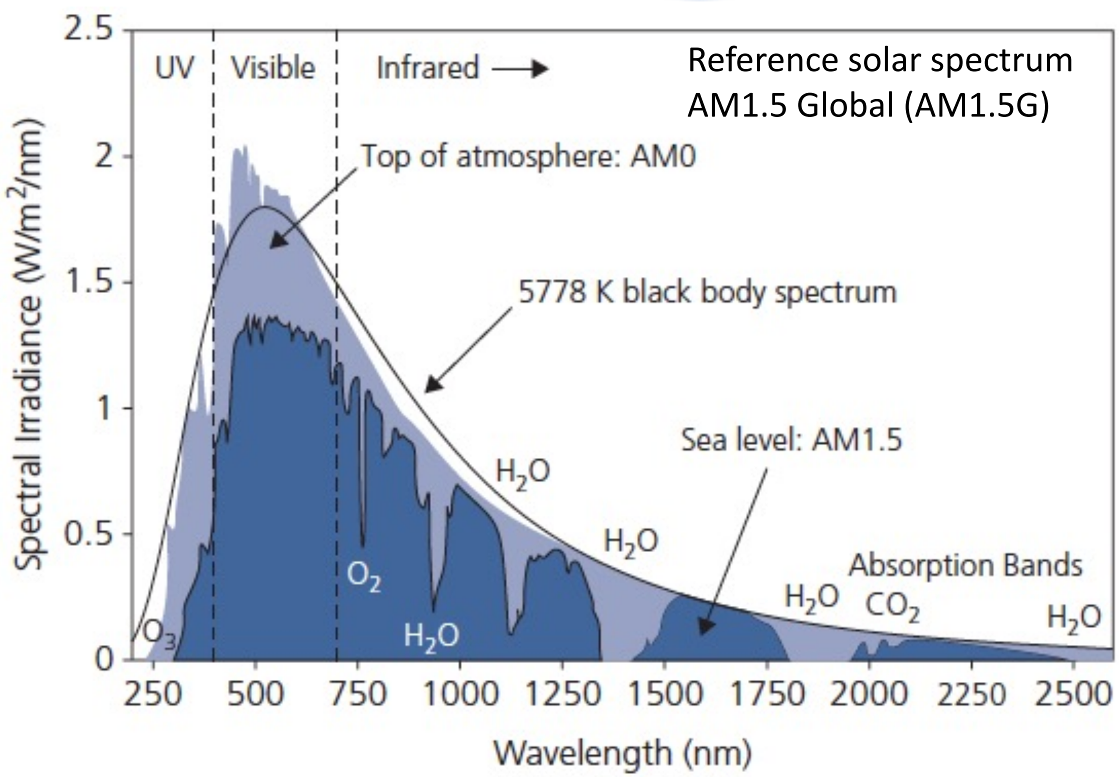

# Annual Solar Insolation: US

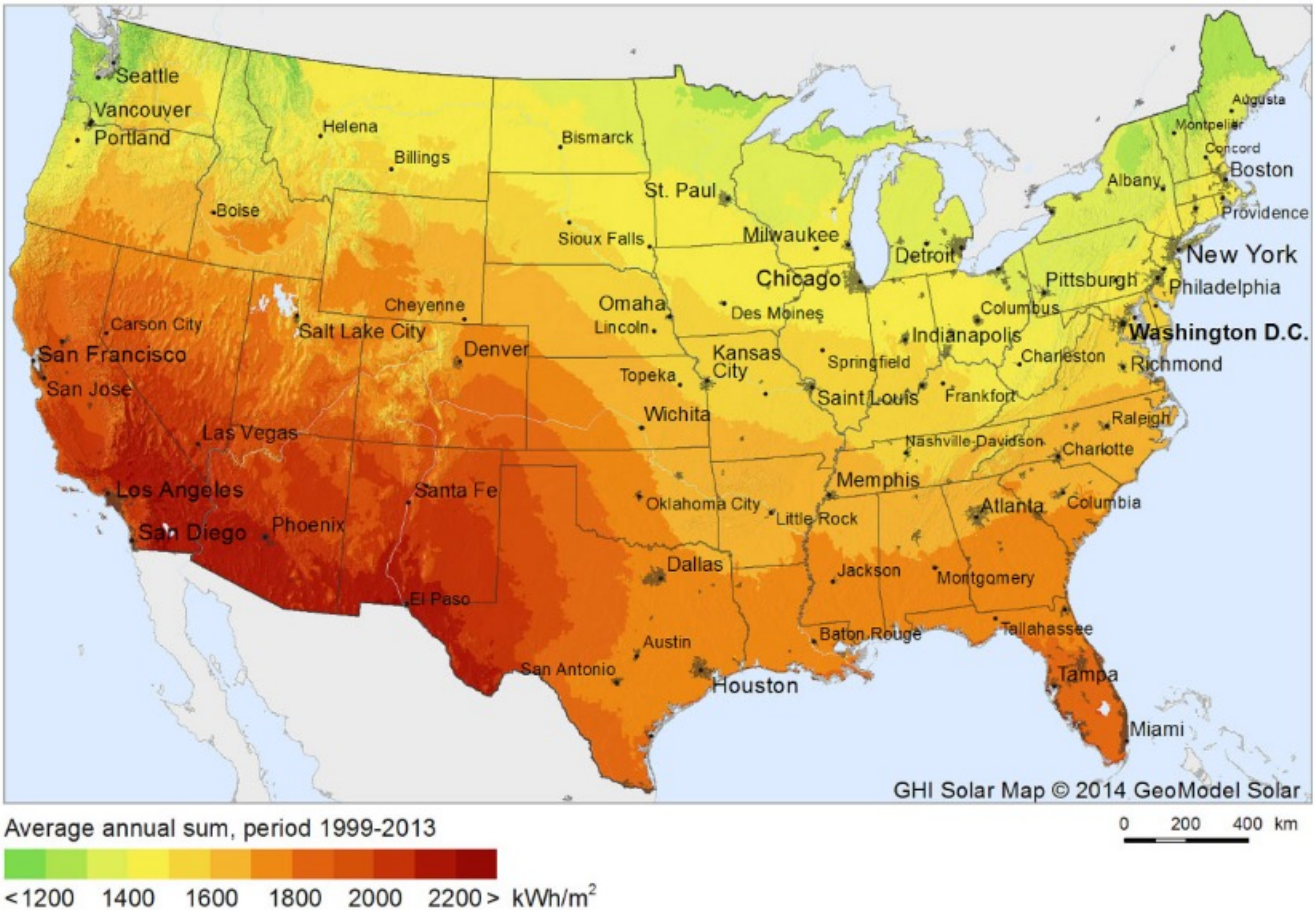


ic Electronics
hen R. Forrest

# Measuring *Single Junction* Solar Cell Efficiency

Challenges:

- The laboratory spectrum ($E_{REF}$) is not identically equal to the reference solar spectrum (AM1.5G):
  It is only simulated ($E_{SIM}$)
- Reference detector spectral response ($S_{REF}$) not identical to the test solar cell ($S_T$)

Example spectra:

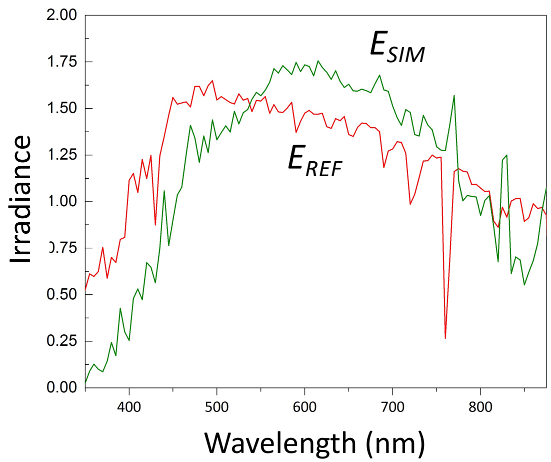


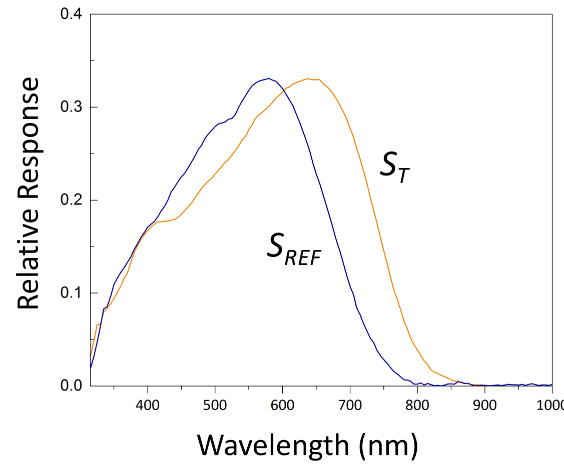


To correct for these differences we calculate the *spectral mismatch factor*

$$M = \frac{j_{SIM}^{T}}{j_{REF}^{T}}\frac{j_{REF}^{REF}}{j_{SIM}^{REF}} = \frac{\int_{\lambda_1}^{\lambda_2} E_{SIM}(\lambda)S_T(\lambda)d\lambda \int_{\lambda_1}^{\lambda_2} E_{REF}(\lambda)S_{REF}(\lambda)d\lambda}{\int_{\lambda_1}^{\lambda_2} E_{REF}(\lambda)S_T(\lambda)d\lambda \int_{\lambda_1}^{\lambda_2} E_{SIM}(\lambda)S_{REF}(\lambda)d\lambda}$$

$j_{SIM}^{T} = j_{SC}$ of test device using the simulated spectrum at 1 sun

$j_{REF}^{T} = j_{SC}$ of test device using the reference AM1.5G spectrum at 1 sun

... etc.

*M* = 1 if $S_{REF} = S_T$ *or* $E_{REF} = E_T$

Solar cell calibration is then: $j_{REF}^{T} = \frac{j_{REF}^{REF} \bullet j_{SIM}^{T}}{M \bullet j_{SIM}^{REF}}$

For most accurate calibration: $M \cong 1$

# Organic Solar Cell Challenges

- High efficiency (>17%)
- Large Module Size
- High Reliability (>20 years)
- Low Production Cost (<$0.50/Watt)

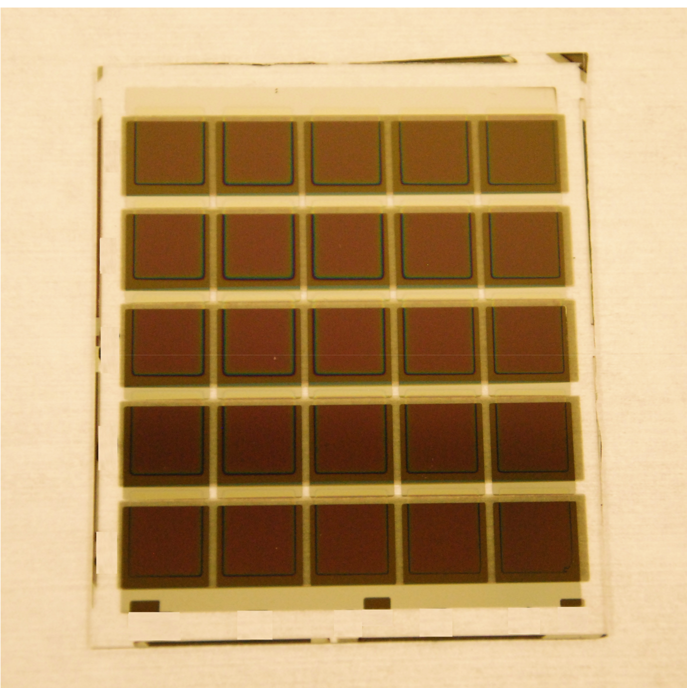

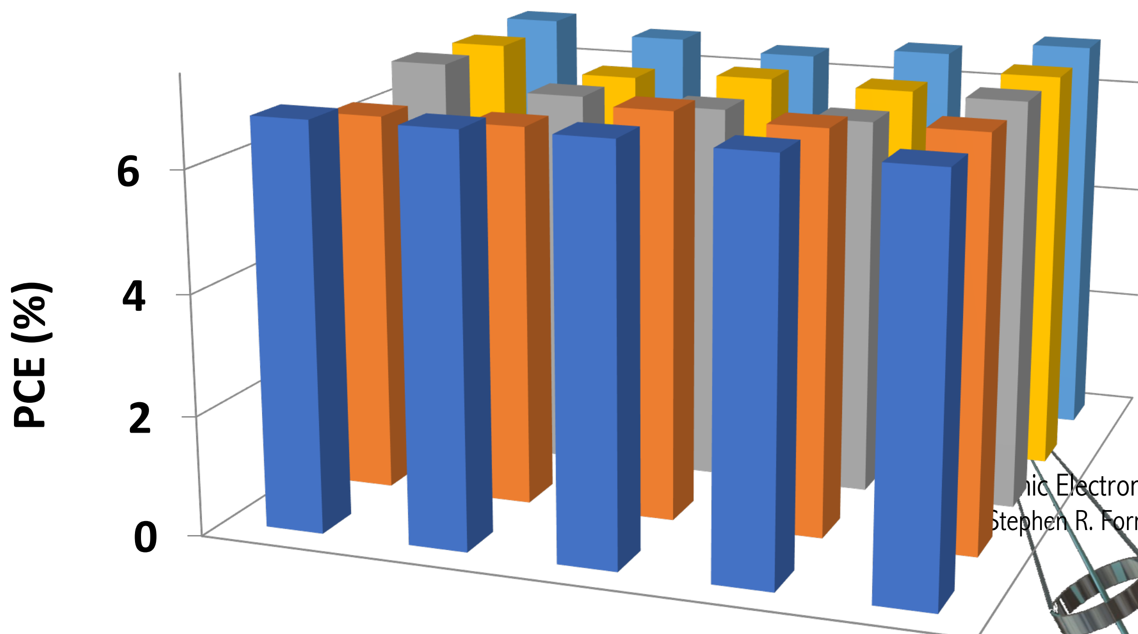

# Getting to High Efficiency: The Double Heterojunction

## Problem

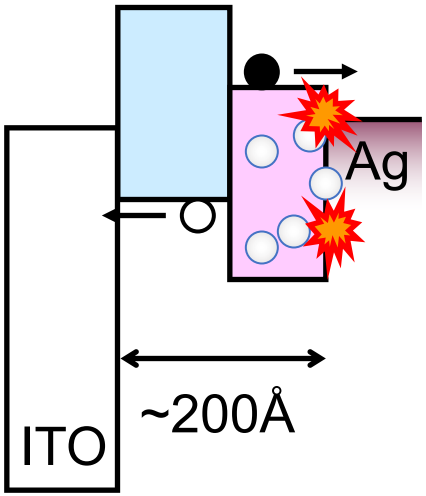


(Tang cell: 1%)

- cathode metal diffusion
- deposition damage
- exciton quenching
- vanishing optical field
- electrical shorts

## Solution

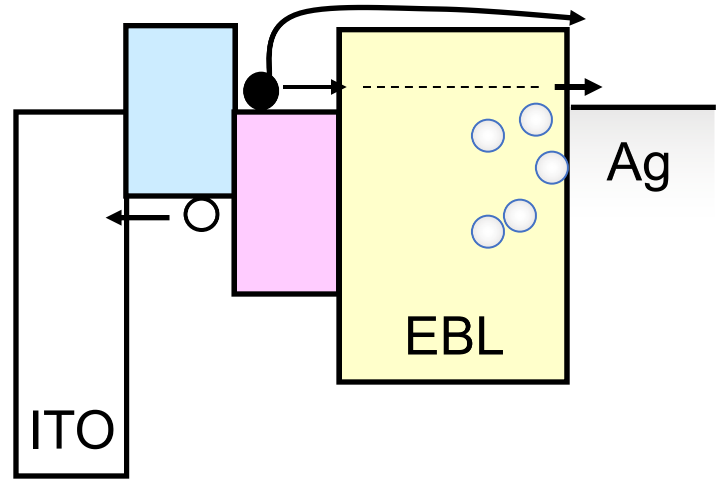


Introduce 'Exciton Blocking Layer' (EBL) to:

- confine excitons to active region
- separates active layer from metal
- act as a buffer to damage
- EBL thickness determined by depth of damage (if too thick, EBL is insulating)

# High efficiency via increased exciton diffusion length: Introduction of fullerenes acceptors

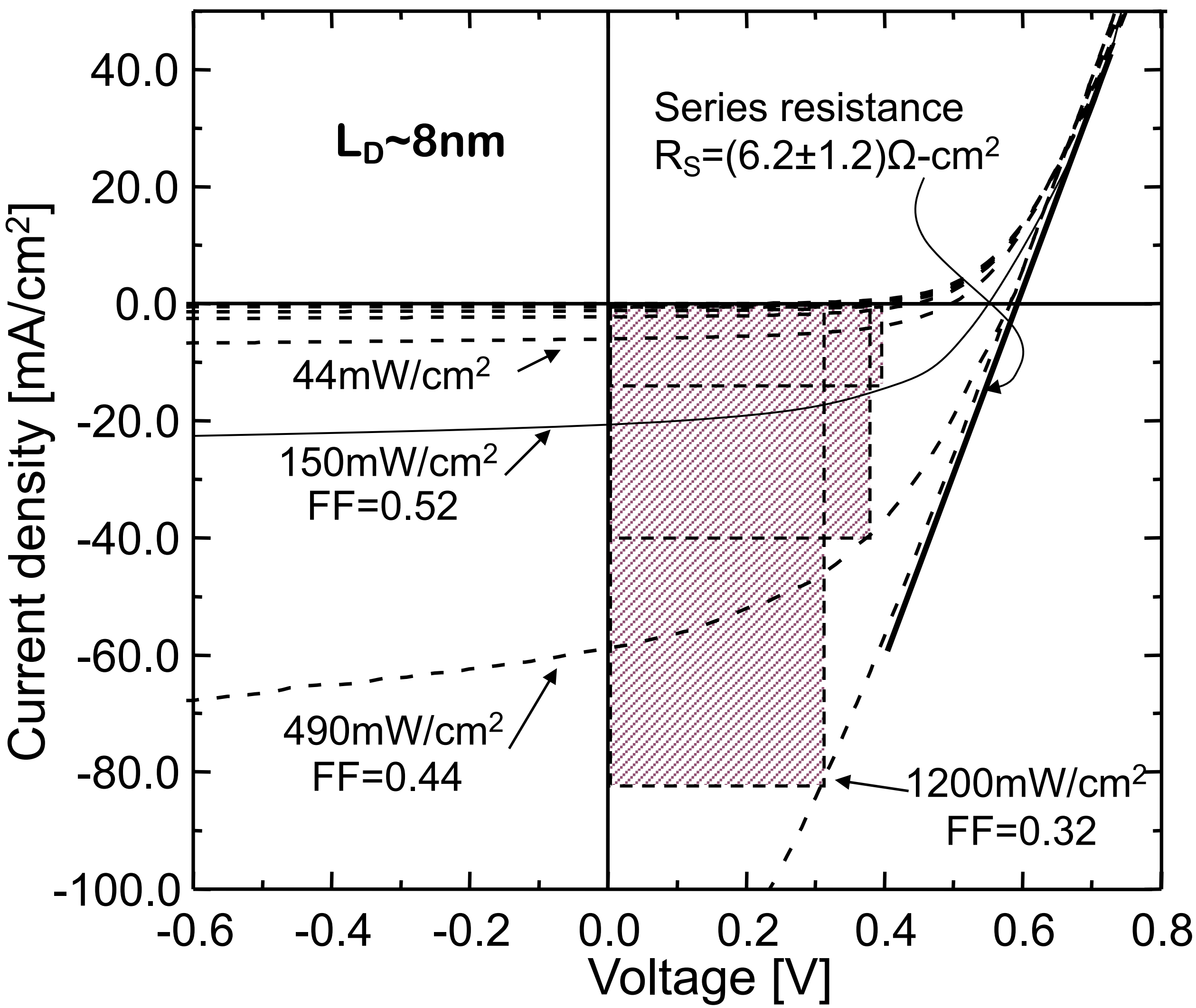


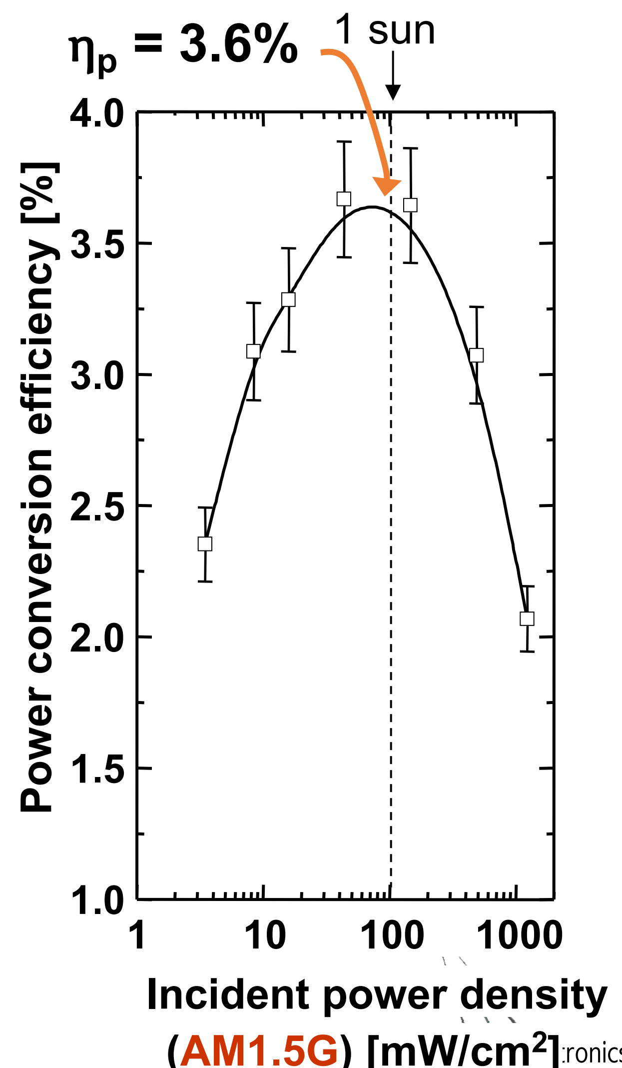


ITO/PEDOT/200Å CuPc/400Å $C_{60}$/**150Å BCP**/800Å Al

Peumans and Forrest., Appl. Phys. Lett., 79,126 (2001)

# Species of Exciton Blockers

- Essential for high efficiency
- Transport charge
- Reduce quenching
- Provides optical spacer
- Reduces damage from Cathode

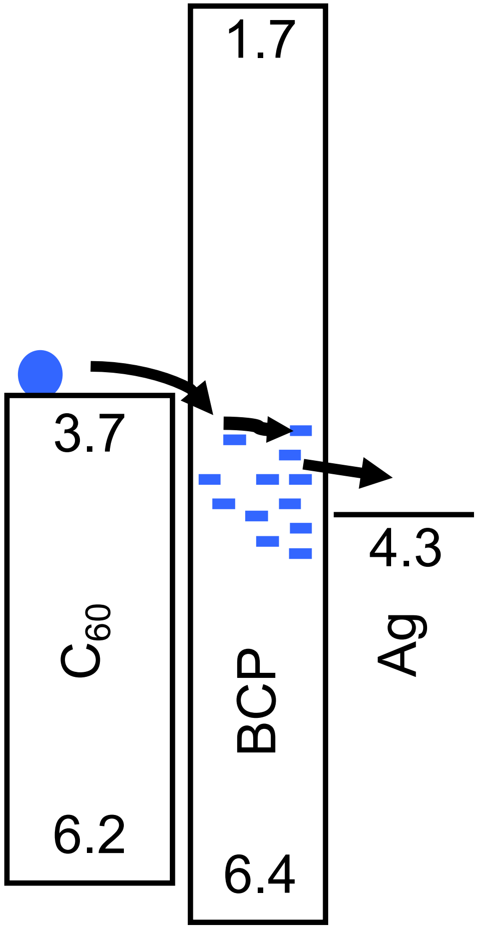


**Trap state transport**

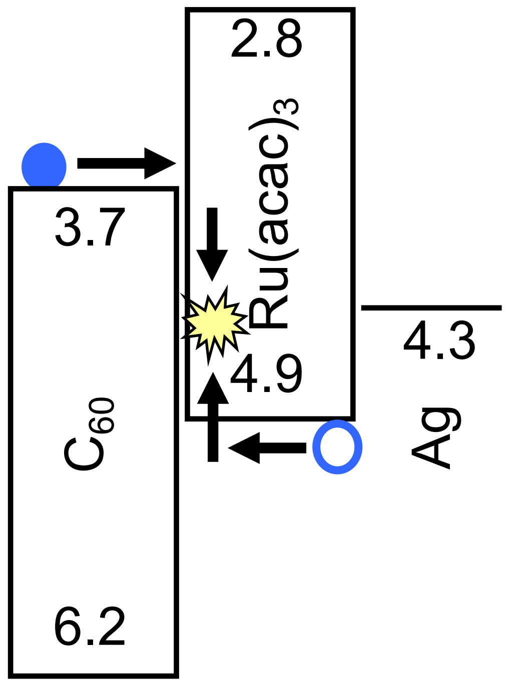


**e-h recombination**

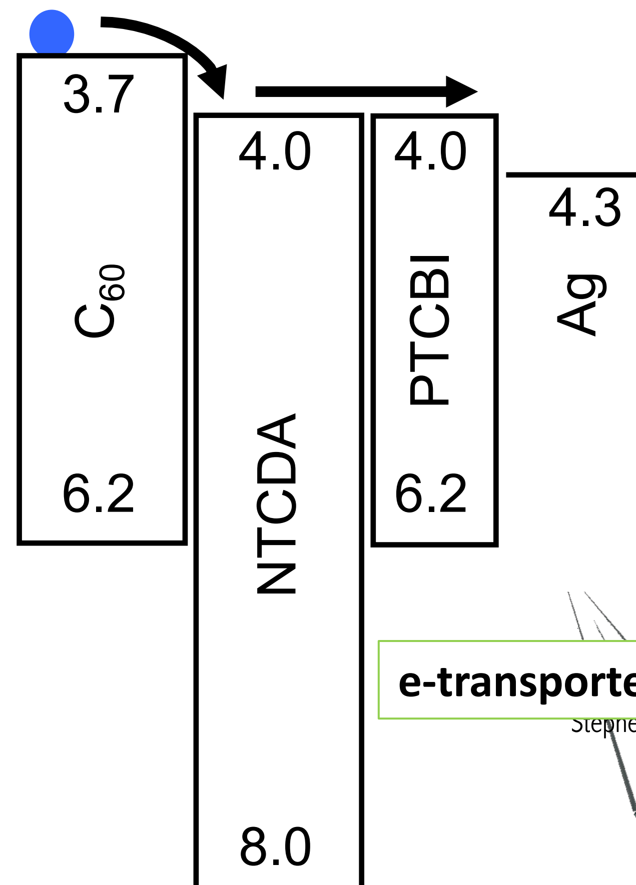


**e-transporter**

Lassiter et al., Appl. Phys. Lett, **98**, 243307 2011

# Electron Filtering Buffer Layer

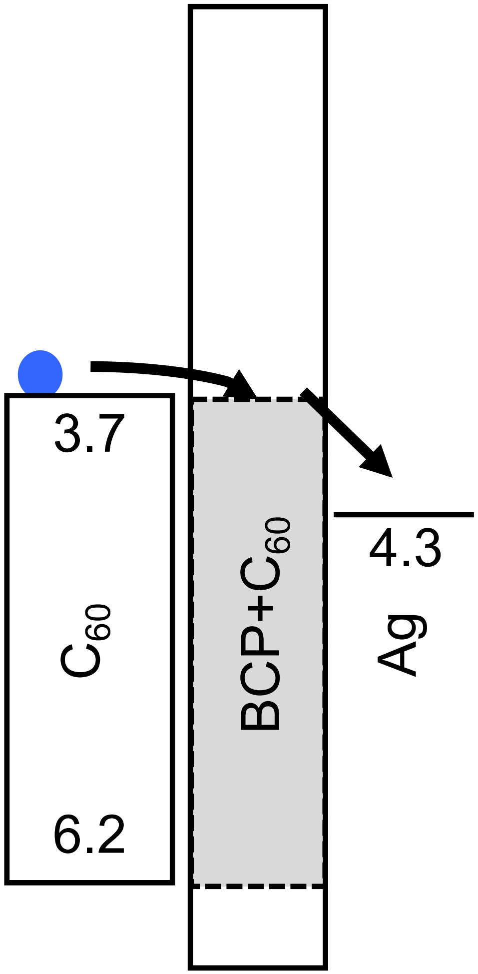


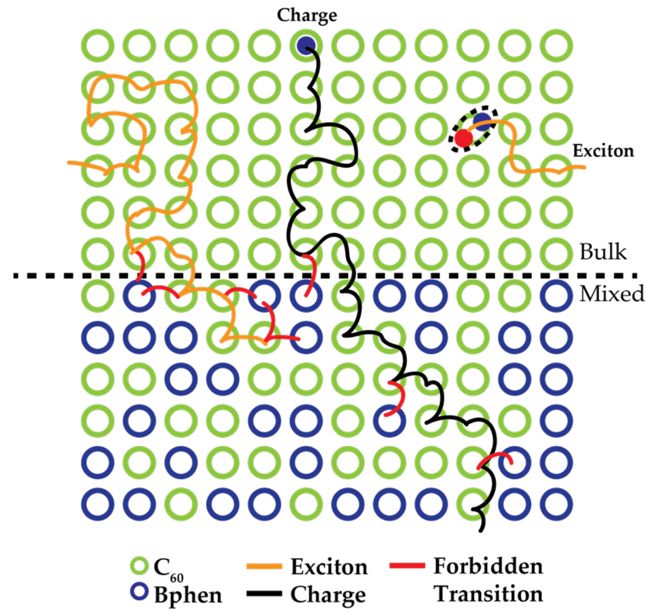


- Highly transparent
- Electron conductivity independent of $C_{60}$ conc. to ~30%
- Compound buffer: $C_{60}$:Bphen/BPhen
- Active region: DBP:$C_{70}$

Bartynski, et al., 13, 3315 Nano Lett (2013)

# $C_{60}$:Bphen Electron Filtering Blockers

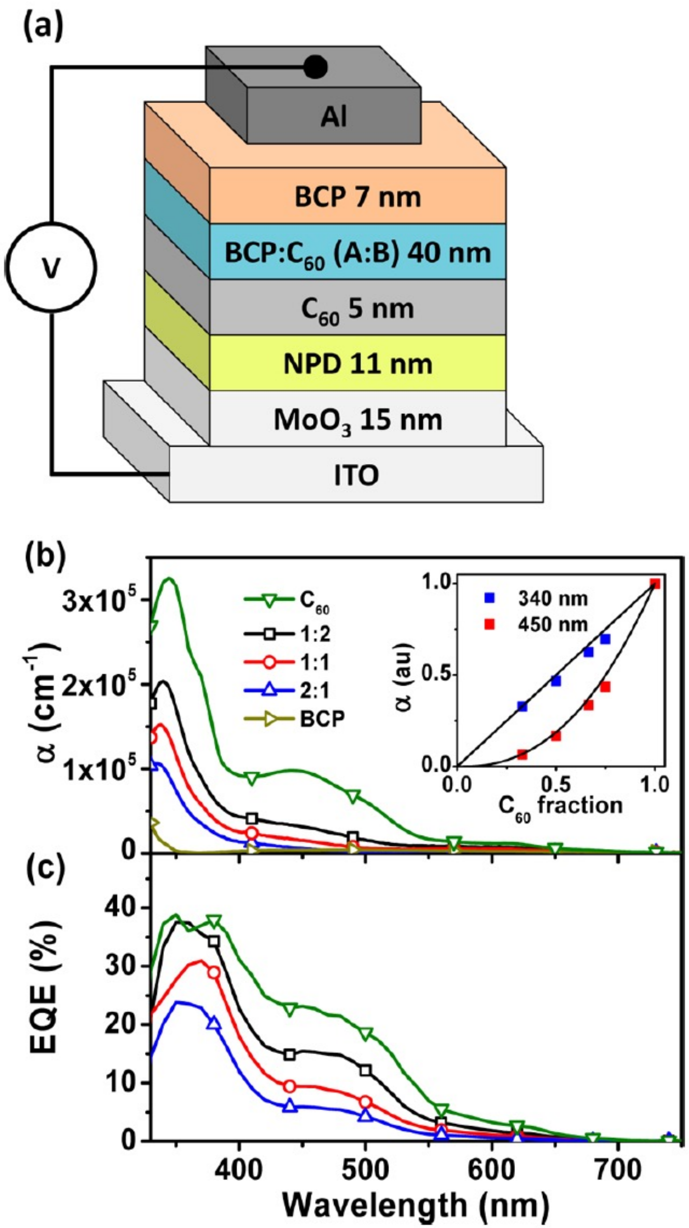


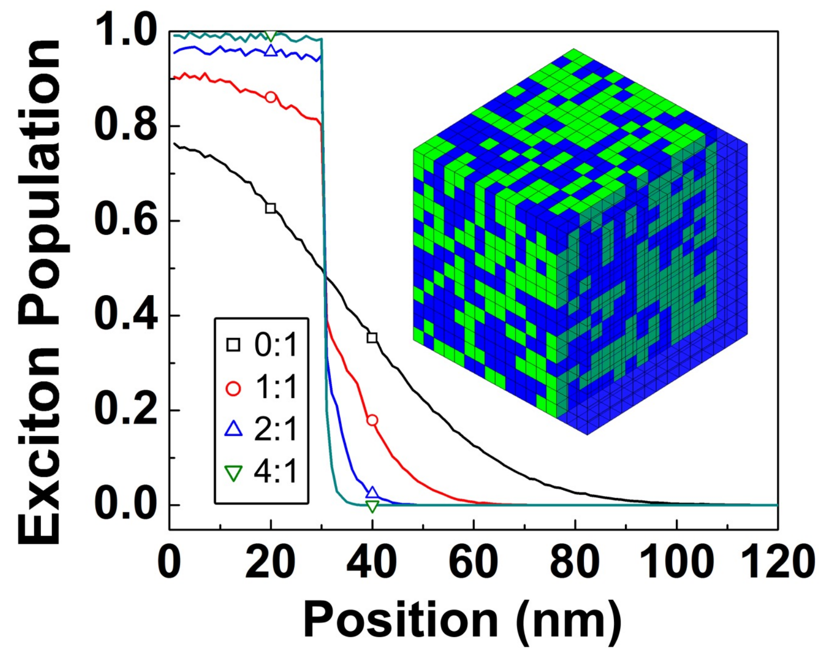


| Doping ($C_{60}$:BCP) | Blocking Efficiency (%) |
|---|---|
| 1:0 | 49.9 ± 0.8 |
| 1:1 | 81.0 ± 0.6 |
| 1:2 | 94.9 ± 0.6 |
| 1:4 | 98.4 ± 0.6 |

Bartynski, et al., 13, 3315 Nano Lett (2013)

# The central importance of morphology

From ideal diode theory

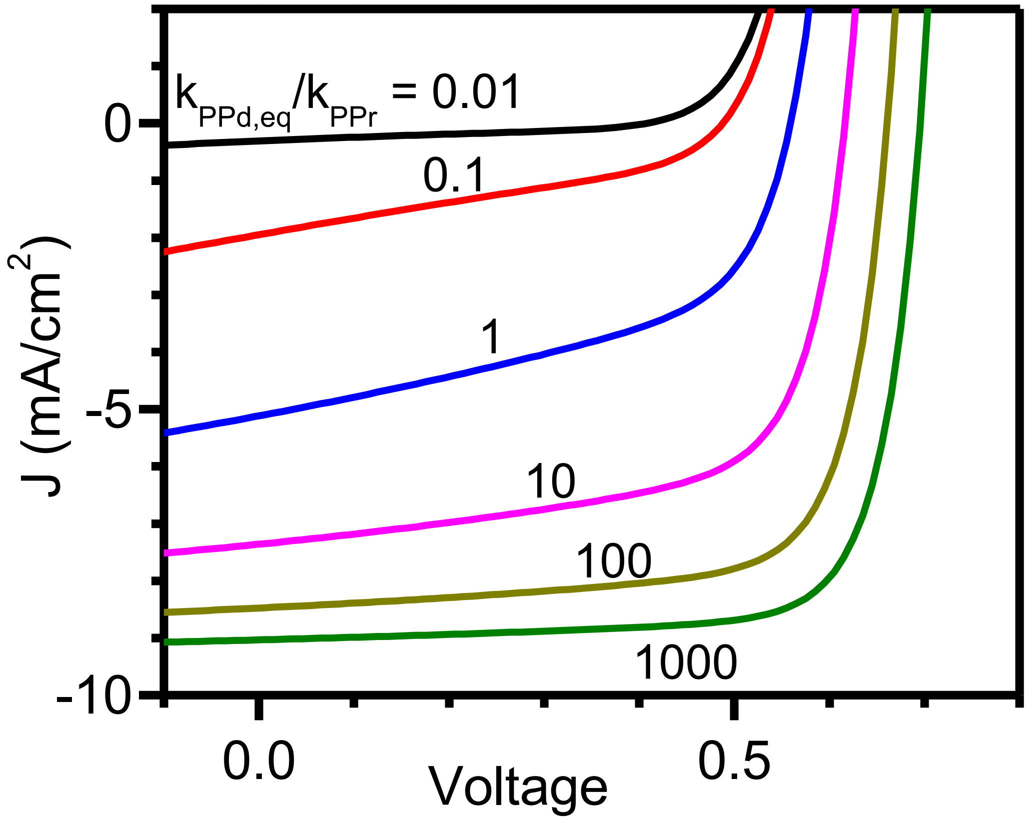


- PP recombination ⇒Reverse Slope
- Best morphologies limit $k_{PPr}$ at interface:
  - **Steric hindrance**
  - **Disorder at interfaces/order in the bulk**

# Open-circuit voltage in OPVs

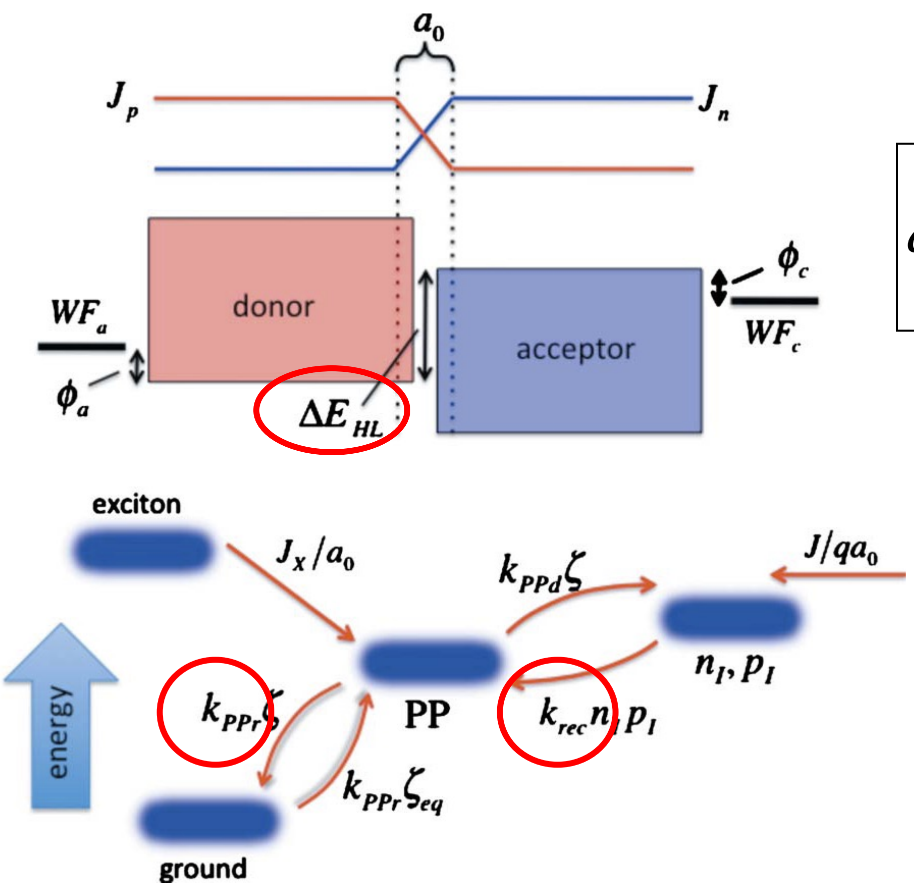


$$qV_{OC} = \Delta E_{HL} - nk_B T \ln\left[\frac{k_{PPr}}{k_{PPd}} \frac{k_{rec} N_L N_H}{J_X / \alpha_0}\right].^*$$

- Material choice determines:
  - $\Delta E_{HL}$ (HOMO-LUMO Gap)
  - Steric hindrance (MO overlap)
- Device processing/morphology can limit $V_{OC}$ losses:
  - $k_{rec}$ (PP formation)
  - $k_{PPr}$ (PP recombination)

*Giebink *et al.* PRB 2010

# Squaraine/Fullerene Solar Cells

## Controlling $k_{ppd}$ via morphology

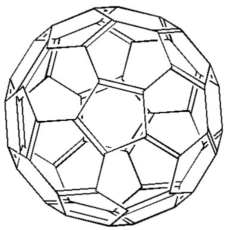

$C_{60}$

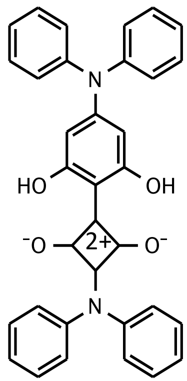


**DPASQ**

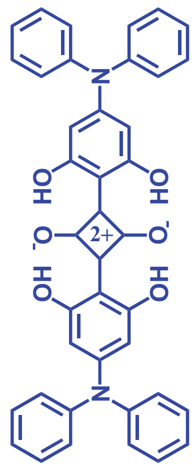


**DPSQ**

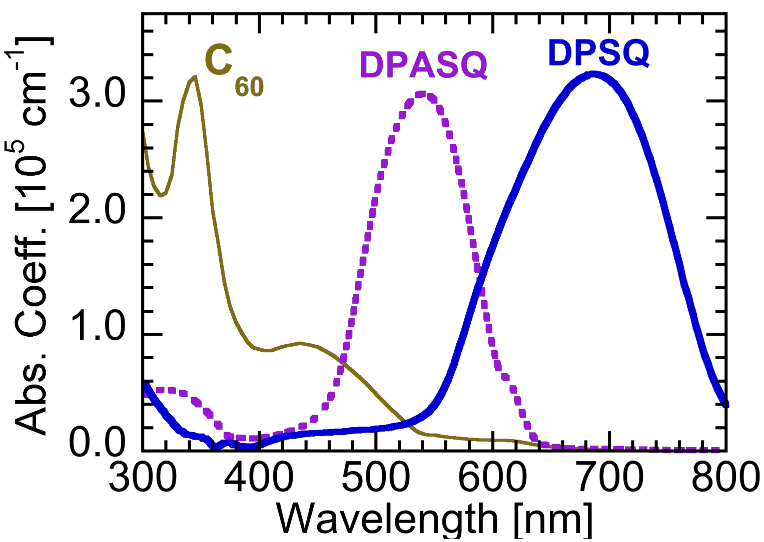


- Squaraines:
  - Very large absorption coefficient.
  - Favorable HOMO/LUMO energies.
  - Large $V_{OC}$.
  - Excellent transport.
  - Simple synthesis.
  - Must be solution processed.
- Bilayer devices:
  - Simplicity allows study of fundamental processes.

# DPSQ Device Structure

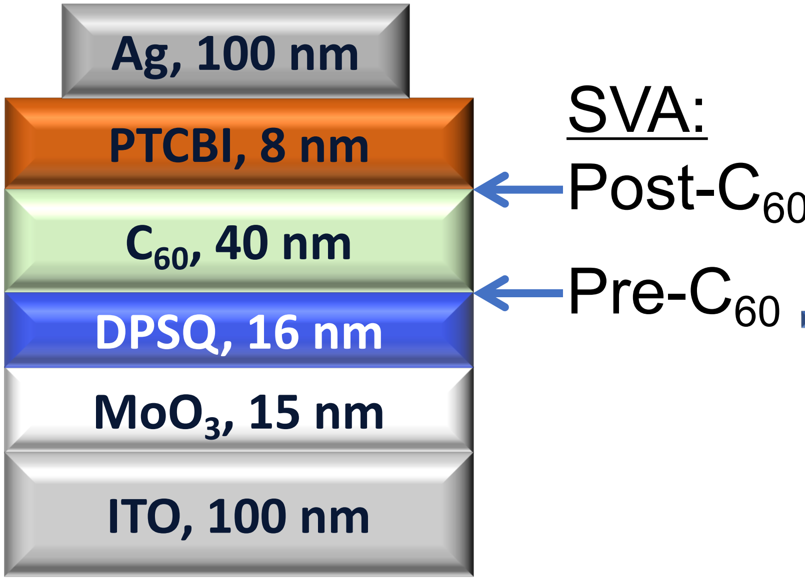


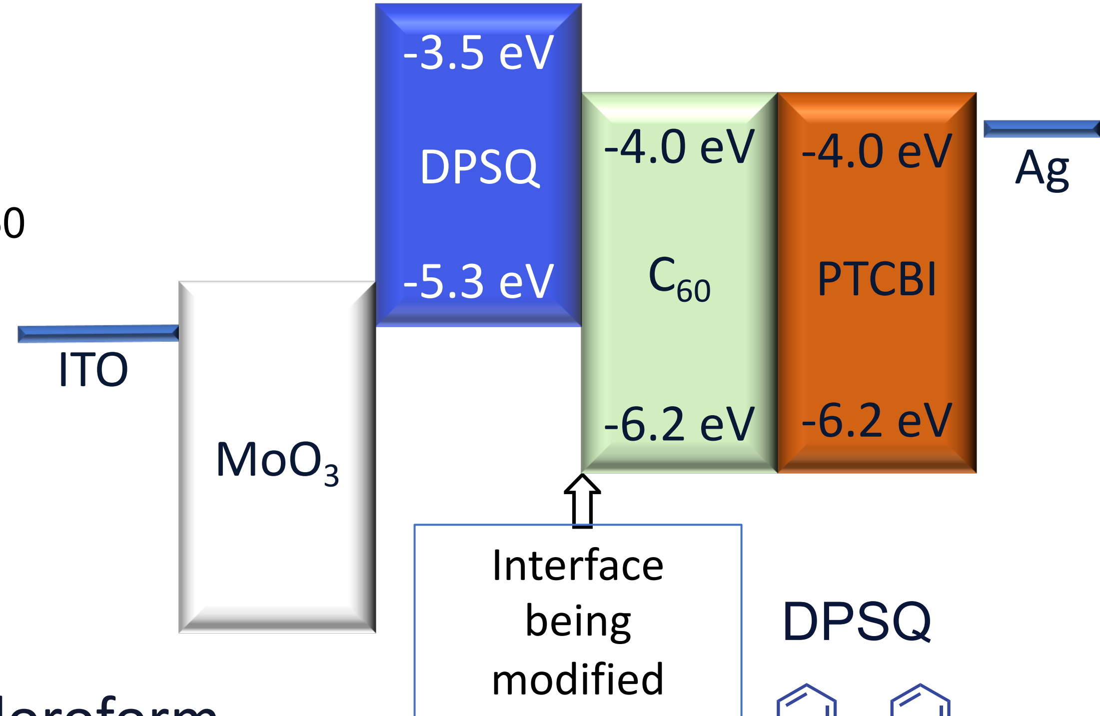


DPSQ

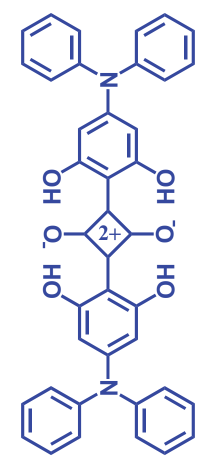


- DPSQ is spun cast from chloroform.
- Other layers deposited by thermal evaporation.
- **Solvent vapor annealing** (SVA):
  - 10 min exposure to a saturated dichloromethane vapor for to "anneal" squaraine component.

# SVA Pre-$C_{60}$

**As Cast DPSQ**

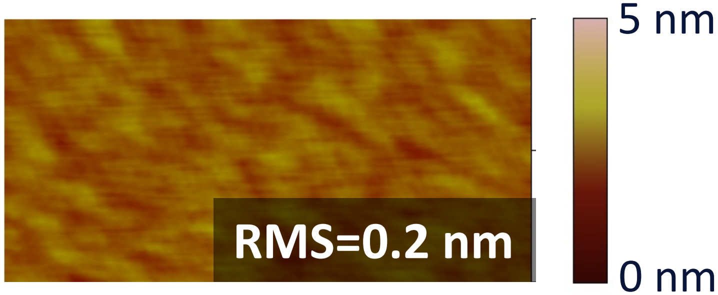


**DPSQ SVA pre-$C_{60}$**


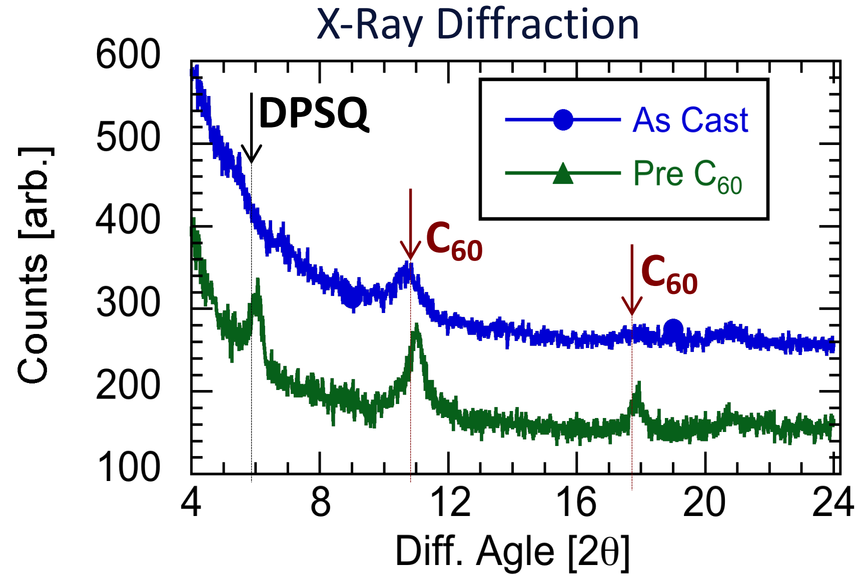


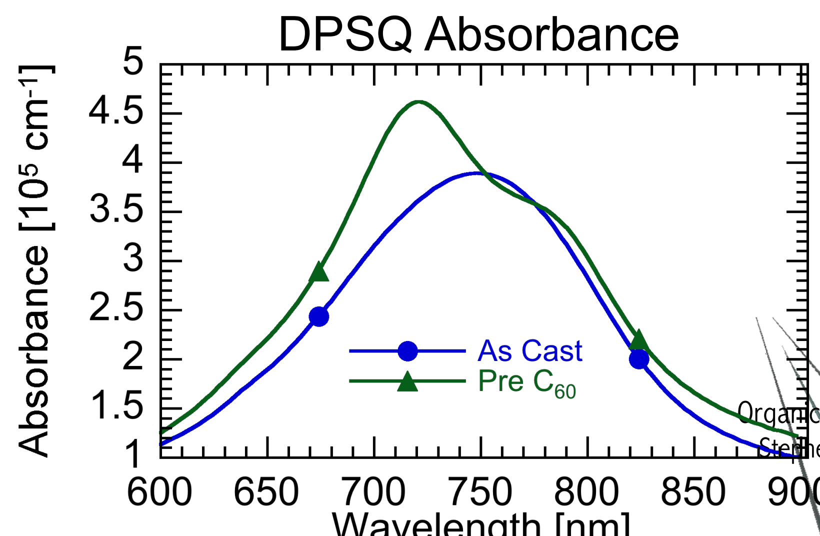


- SVA Pre $C_{60}$:
  - Crystallizes and roughens DPSQ.
  - Crystalline DPSQ templates *quasi-epitaxial* $C_{60}$ growth.

# Devices SVA Post-$C_{60}$

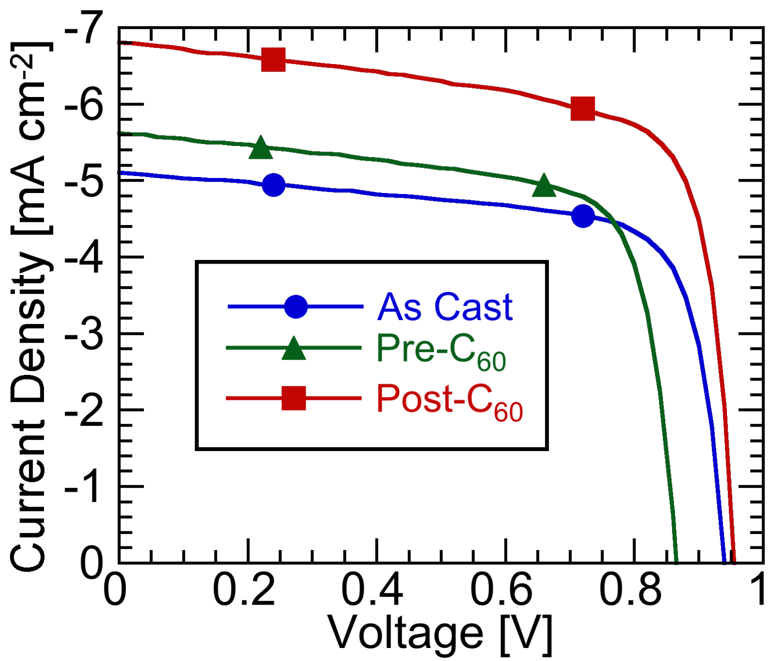


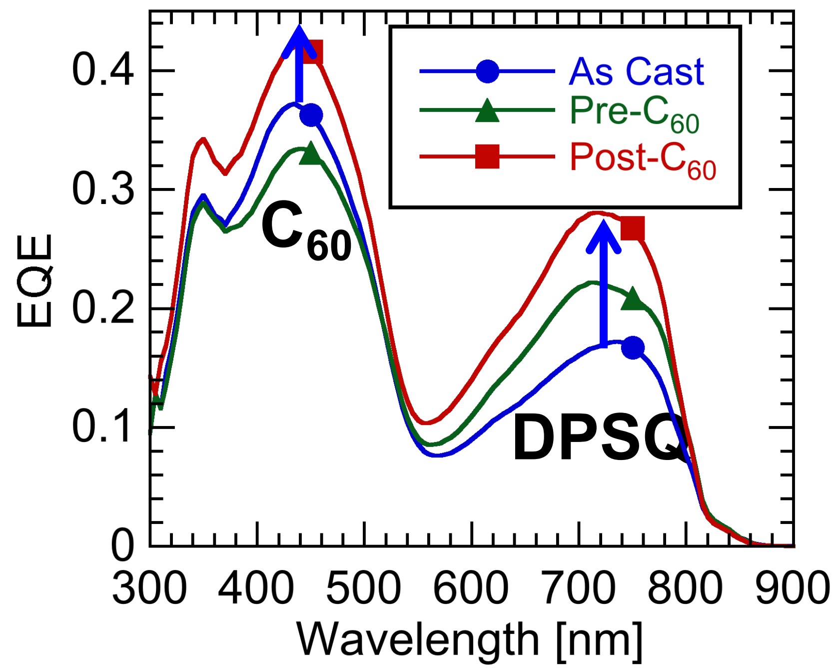


- SVA post-$C_{60}$
  - DPSQ EQE ⇧80%.
  - $J_{SC}$ ⇧25%.
- No loss in $V_{OC}$
  - $k_{PPr}$ unchanged.

| Process | $J_{SC}$[mA cm$^{-2}$] | $V_{OC}$ [V] | FF [%] | $\eta_P$ [%] |
|---|---|---|---|---|
| As Cast | 5.3±0.3 | 0.94 | 73 | 3.6±0.2 |
| Pre-$C_{60}$ | 5.6±0.3 | 0.86 | 70 | 3.4±0.2 |
| Post-$C_{60}$ | 7.0±0.4 | 0.96 | 71 | 4.8±0.3 |

# Achieving the Ideal Morphology

| $C_{60}$<br>DPSQ | 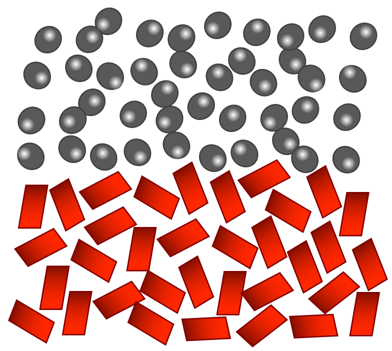 | 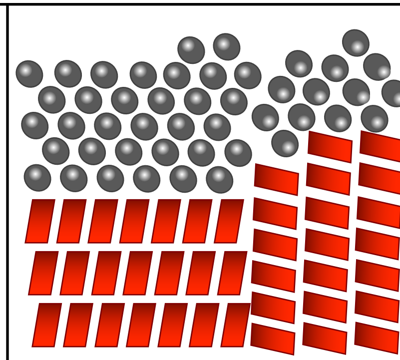 | 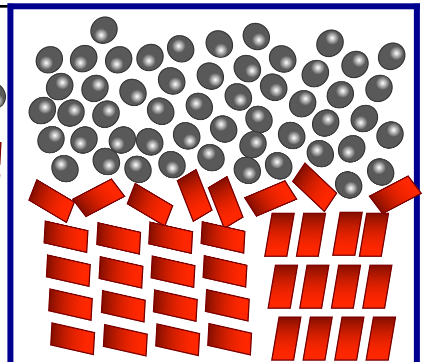 |
|---|---|---|---|
| | **As Cast** | **Pre $C_{60}$** | **Post $C_{60}$** |
| Bulk DPSQ | Amorphous | Ordered | Mod. Order |
| Bulk $C_{60}$ | Weak order | Ordered | Weak Order |
| Interface | Disordered | Ordered | Disordered |
| Surface | Smooth | Rough | Smooth |
| $k_{PPr}$ | Low | High | Low |
| $V_{OC}$ | High | Low | High |
| $J_{SC}$ | Low | Moderate | High |

nic Electronics
phen R. Forrest

J. D. Zimmerman, et al. Nano Lett. (2012)

# Morphology vs. $V_{OC}$

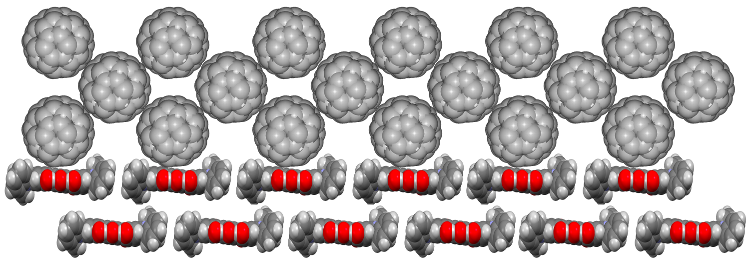

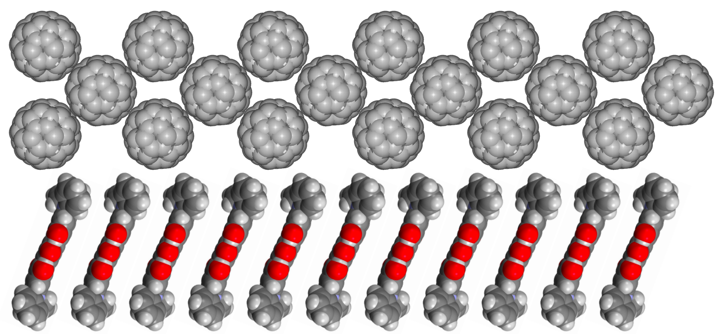

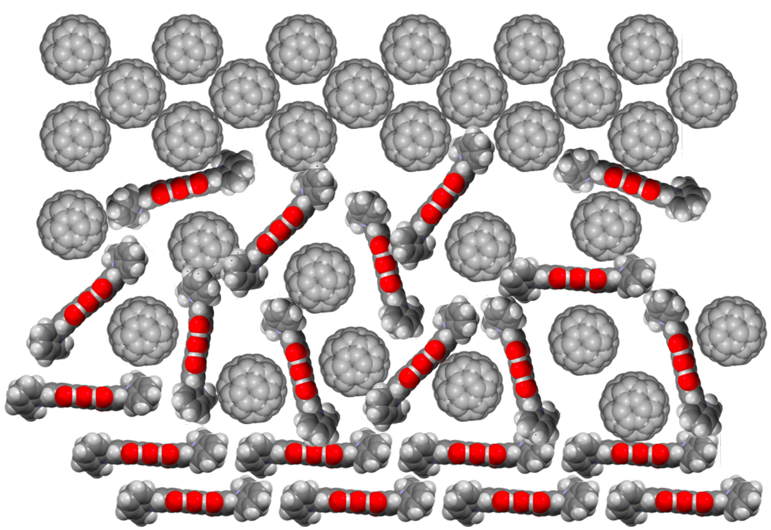

$$qV_{OC} = \Delta E_{HL} - nk_B T \ln\left[\frac{k_{PPr}}{k_{PPd}} \frac{k_{rec} N_L N_H}{J_X / \alpha_0}\right]$$

$$k_{rec} = \gamma = \frac{q}{\varepsilon}\left(\mu_e + \mu_h\right)$$

- Worst case scenario: perfectly ordered crystalline interface and bulk, Face-on .
  - High $k_{PPr}$ and $k_{rec}$
- Better Scenario I: Perfectly crystalline and end-on orientation
- Even Better Scenario II: crystalline bulk, intermixed interface
  - Poor coupling between like-molecules ($C_{60}$-$C_{60}$ and SQ-SQ) reduces PP formation ($k_{rec}$) probability.
  - Overcomes enhanced $k_{PPr}$ due to facial contact

# Increasing solar coverage: Exciton Cascades

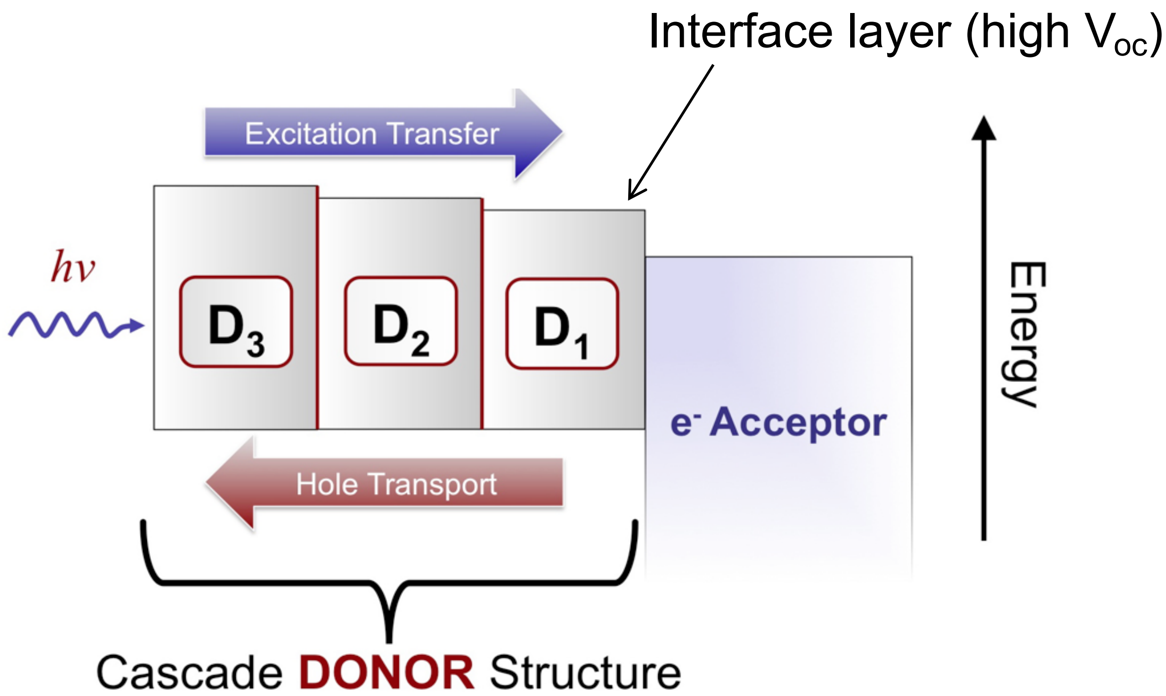


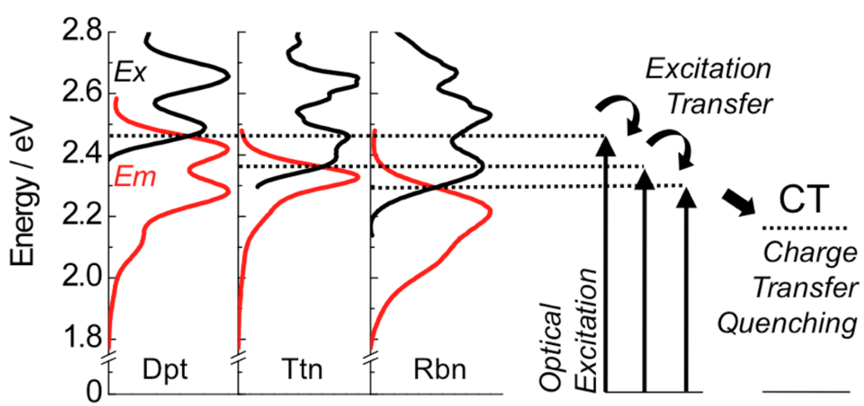


Schlenker, et al., *Chem. Mater.*, **23**, 4132 (2011).

# High Efficiency Donor Cascade Device

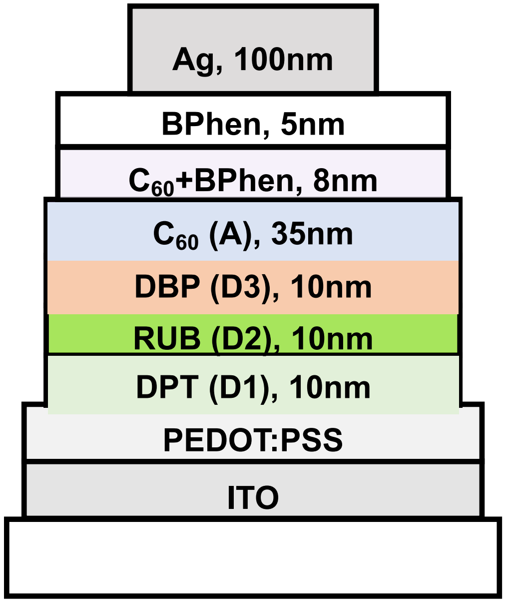


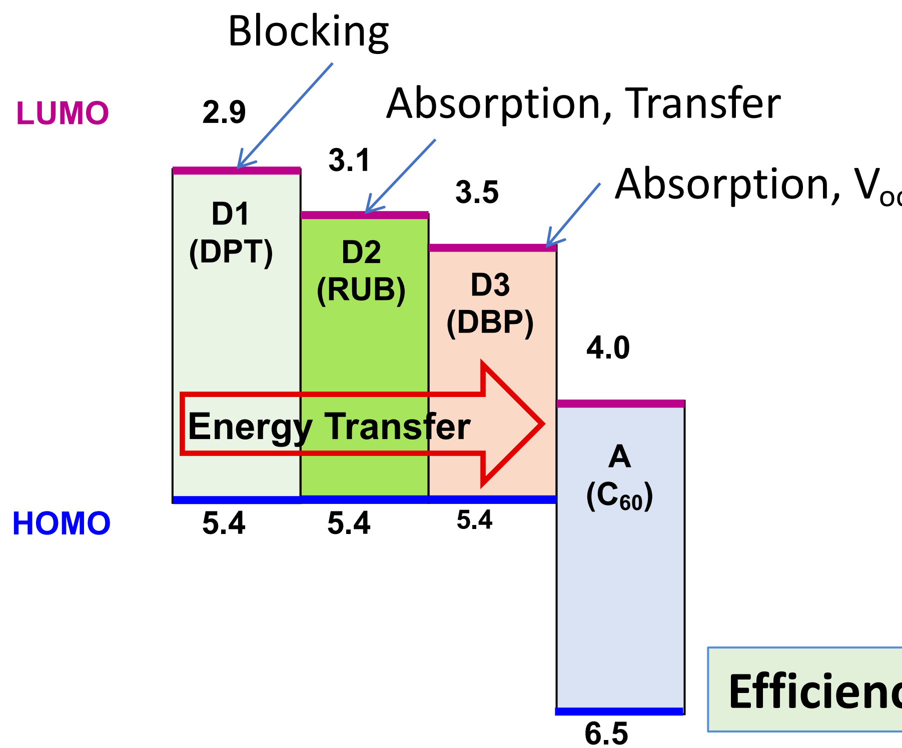


**Efficiency: 7.1%**

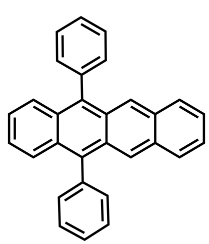

**DPT**

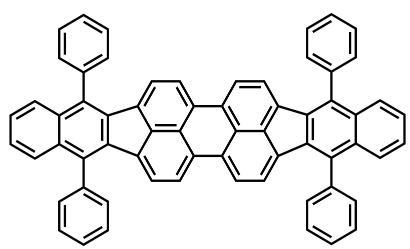

**DBP**

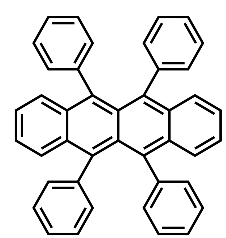

**RUB**

O. L. Griffith & S. R. Forrest, *Nano Letters*, 14, 2353 (2014).

# Ternary BHJs Increase Solar Coverage

Charge Xfer

Energy Xfer

Parallel Junctions

"Alloy" formation

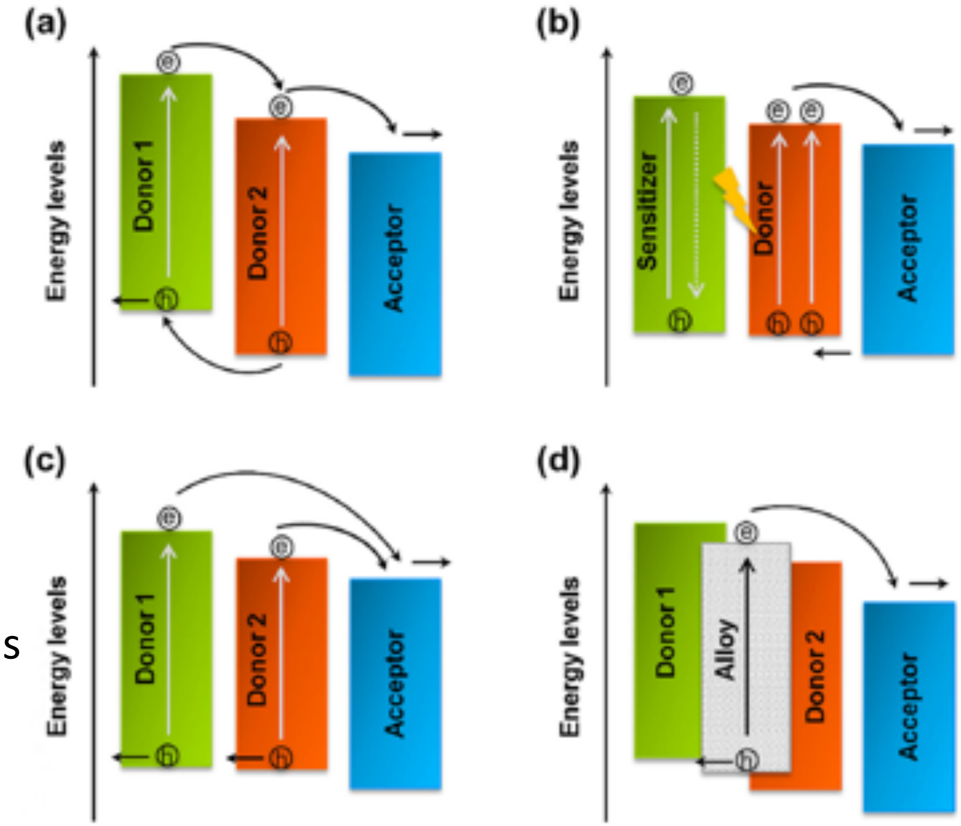


**Features of ternary blends:**

- $V_{OC}$ of the ternary lies between the extremes of the two subcell junctions
- Materials chosen to cover solar spectrum
- Can be $DA_1A_2$ or $AD_1D_2$ junctions
- Morphology is key
- Probably more than one process governs performance
- Molecular alloy formation unlikely

# Example $DA_1A_2$ ternary BHJ

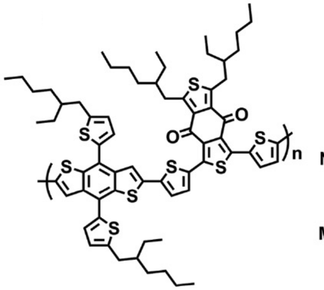



**PBDB-T**

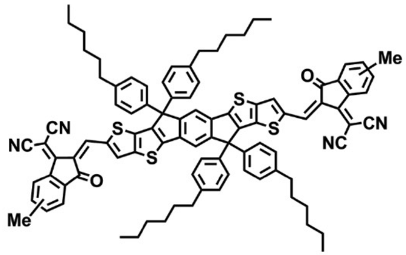



**IT-M**

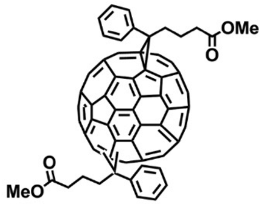



**$BisPC_{71}BM$**

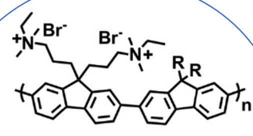



$R=C_8H_{17}$

**PFN-Br**

Exciton blocker

| $D:A_1:A_2$ ratio | $V_{OC}$ (V) | $j_{SC}$[(a)] ($mA/cm^2$) | *FF* | $\eta_P$ (max) (%) | $\eta_P$ (ave)[(b)] (%) |
|---|---|---|---|---|---|
| 1:1:0 | 0.937 | 16.7 | 0.69 | 10.80 | 10.45 |
| 1:1:0.2 | 0.952 | 17.4 | 0.74 | 12.20 | 11.75 |
| 1:0:1 | 1.02 | 10.6 | 0.58 | 6.25 | 5.86 |

- Cell area = 4 $mm^2$.
- Sample size = 100 diodes

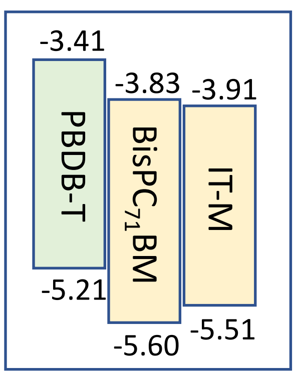



W. Zhao, et al., *Advanced Materials,* **29**, 2, 2017.

# Bi-ternary OPV

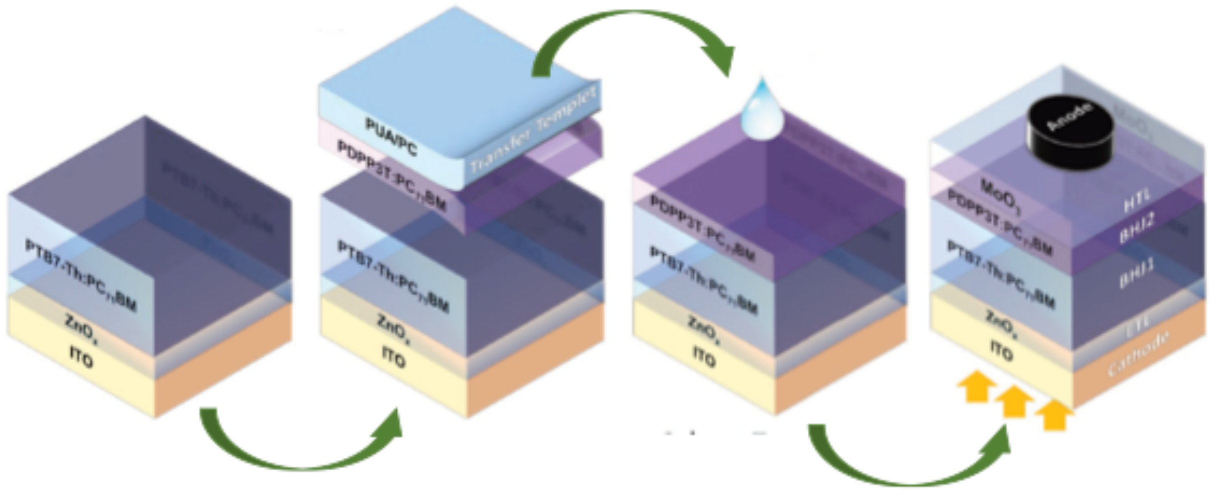


Intermixing of two donors creates continuous hole and electron conduction

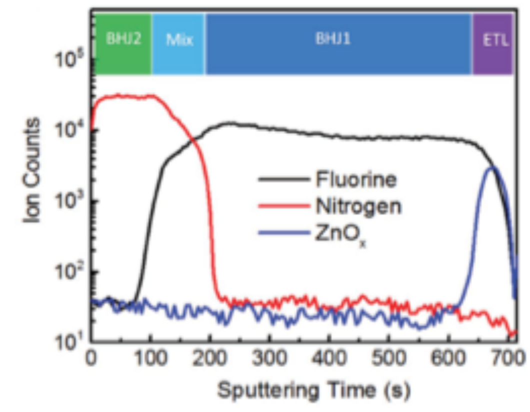


| Cell[a] | $V_{OC}$ (V) | $j_{SC}$[b] (mA/cm²) | *FF* | $\eta_P$ (max) (%) | $\eta_P$ (ave)[c] (%) |
|---|---|---|---|---|---|
| BHJ1 | 0.81 | 18.5 | 0.70 | 10.5 | 10.3 |
| BHJ2 | 0.69 | 7.4 | 0.71 | 3.6 | 3.5 |
| BHJ1/2 | 0.77 | 23.8 | 0.67 | 12.3 | 11.9 |

(b)

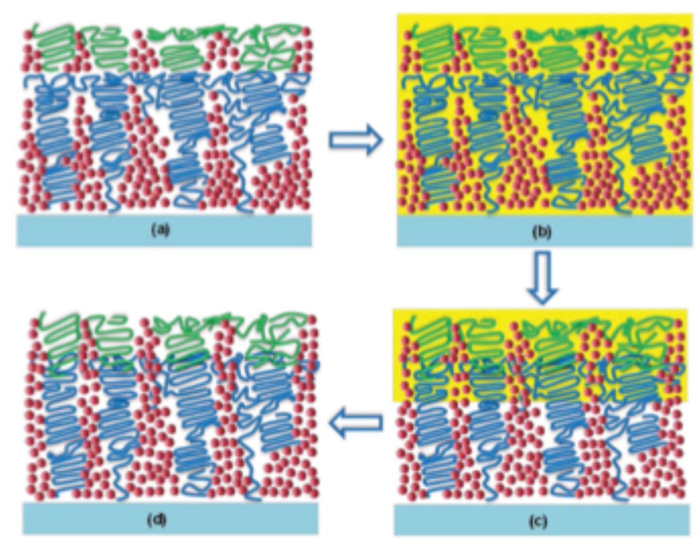


J. Huang, *Advanced Materials*, **29**, 1606729, 2017.

# Wavelength-selective Absorption Can Lead to Semitransparent OPVs

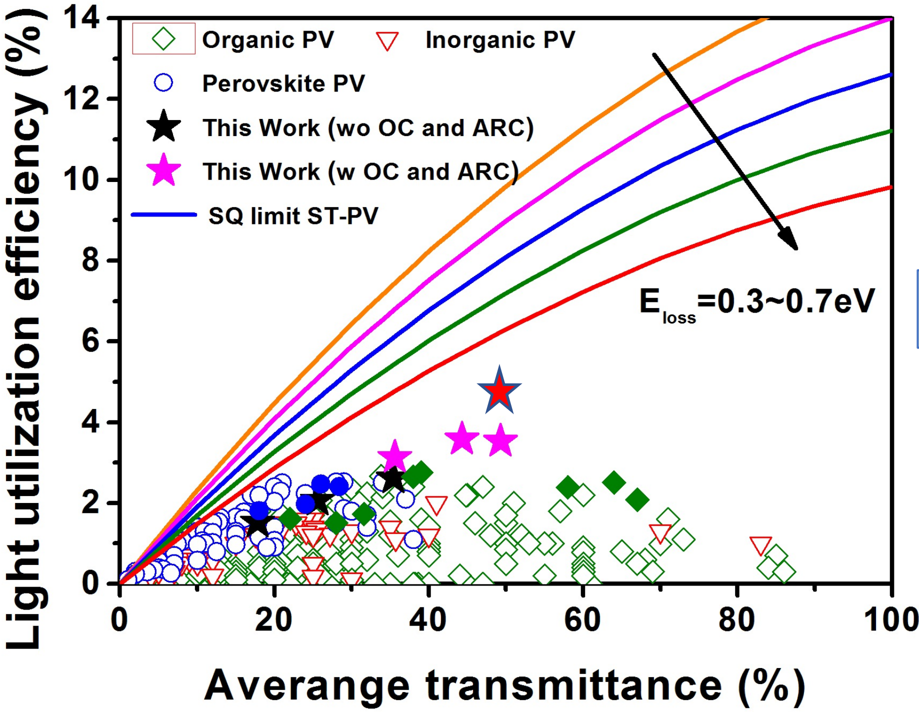


Power generating windows (transparent in the visible, absorbing in the NIR) are a major opportunity unique to OPVs

Transparent OPV Figure of Merit

$$LUE = PCE \times APT$$

$LUE$: light utilization efficiency

*PCE:* power conversion efficiency

*APT:* average photopic transmission

$$\boldsymbol{APT} = \frac{\int T(\lambda)P(\lambda)S(\lambda)d(\lambda)}{\int P(\lambda)S(\lambda)\,d(\lambda)}$$

$\lambda$: wavelength; *T*: transmission

*P:* photopic response; *S*: solar photon flux (AM1.5G)

# Semi-Transparent Device Materials & Structures

## Example of Photon Management

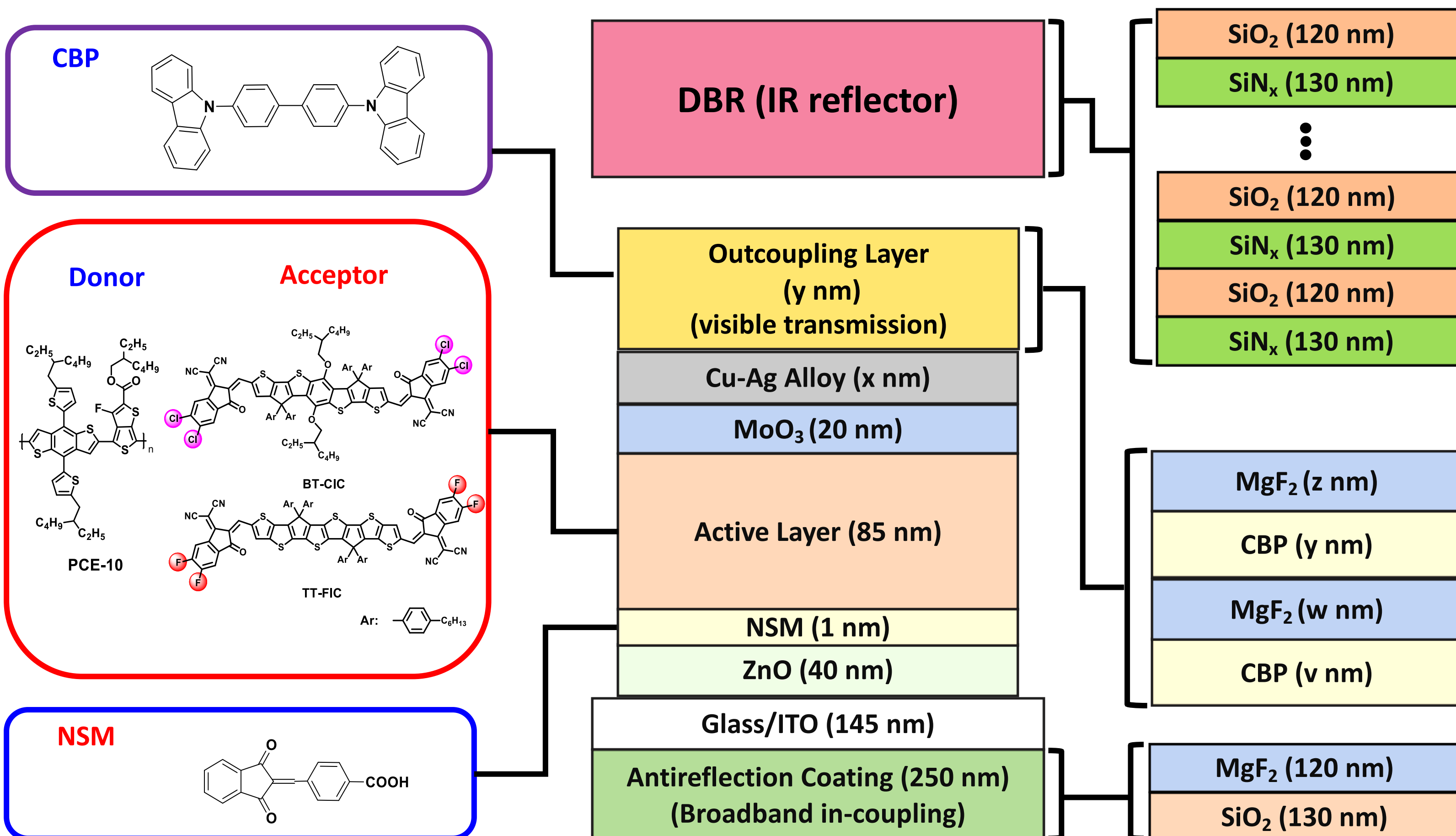


Li, et al. Adv. Mater., 31, 1903173 (2019)

# Non-Fullerene Acceptor Molecular Design

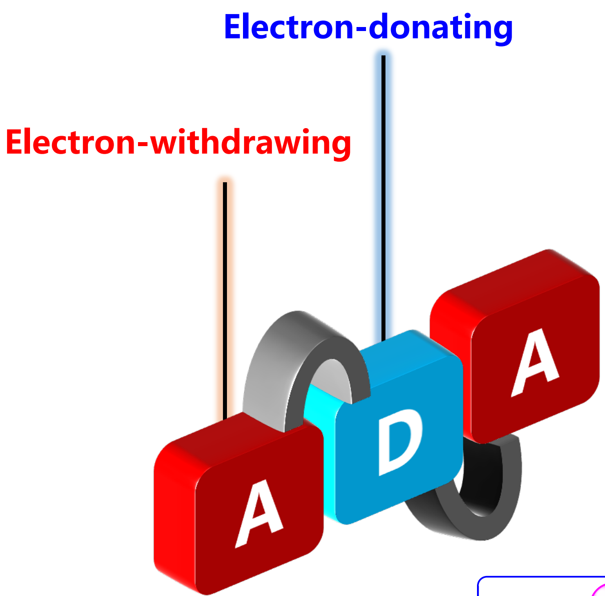


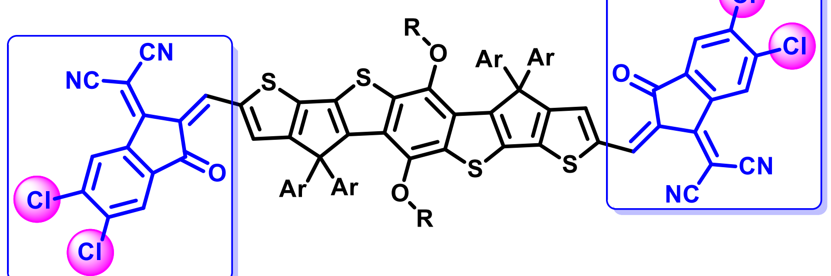


BT-CIC

Absorption tunability presents opportunities unique to OPVs

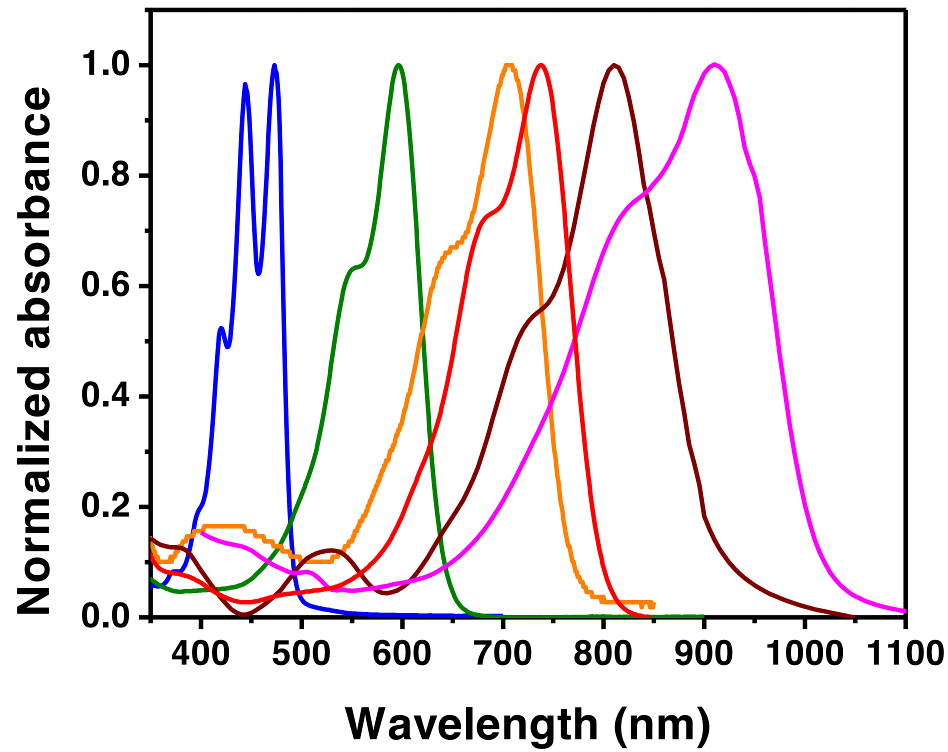


# Semi-Transparent Organic Solar Cells

## Color Tunable Windows

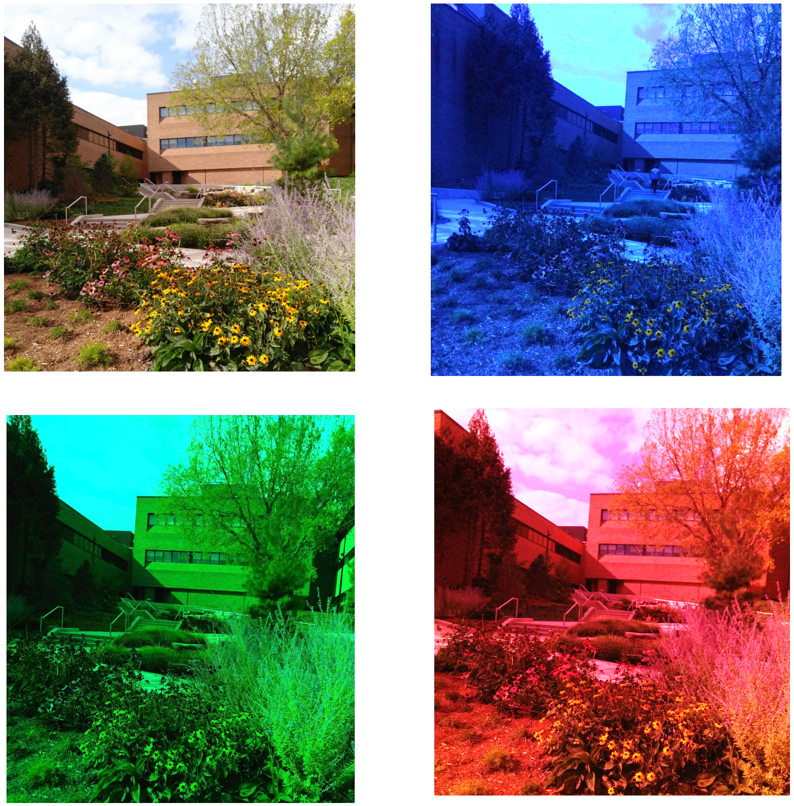

Preferred windows are neutral density

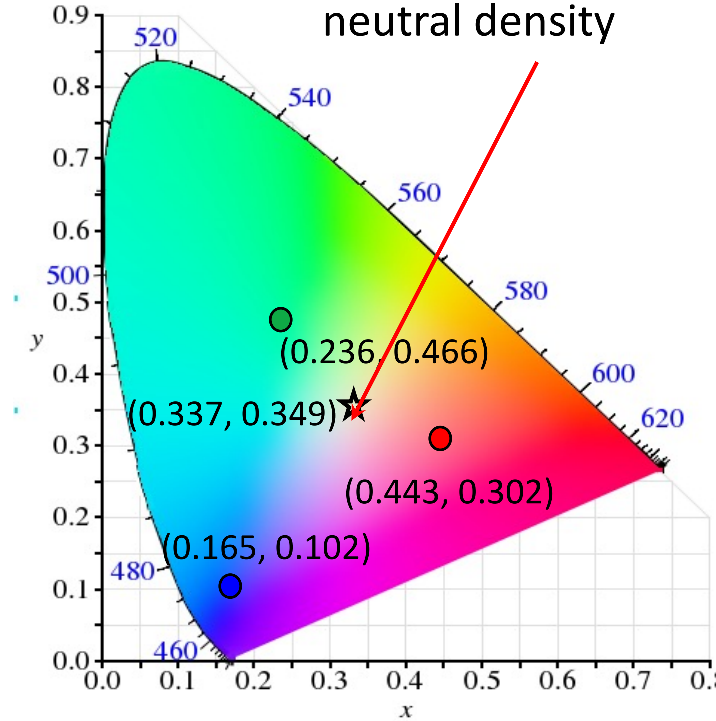


| Active Layer | $J_{sc}$ [mA/cm$^2$] | $V_{oc}$ [V] | FF [%] | PCE [%] |
|---|---|---|---|---|
| **PCE-10:BT-CIC (1:1.5)** | **22.5 (21.3)** | **0.70** | **71.0** | **11.2** |
| **PCE-10:DTD-FIC (1:1.5)** | **25.6 (21.3)** | **0.64** | **69.5** | **11.3** |

Li, et al. Adv. Mater., 31, 1903173 (2019)

# Optical Outcoupling Layers

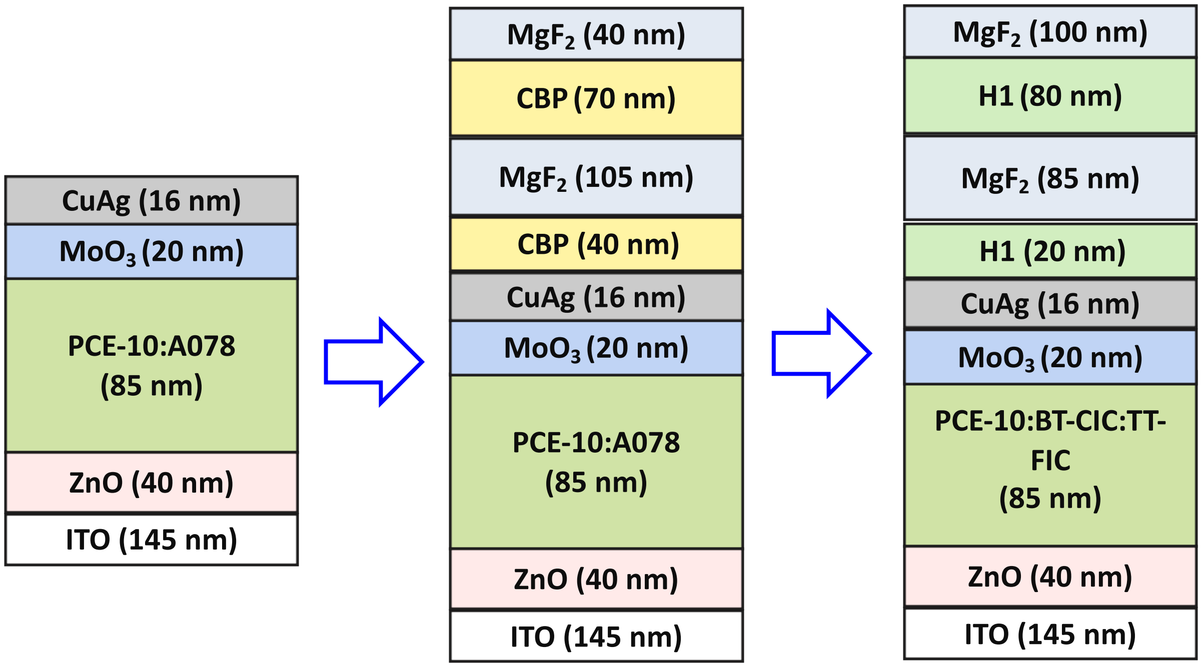


OC-1 OC-2

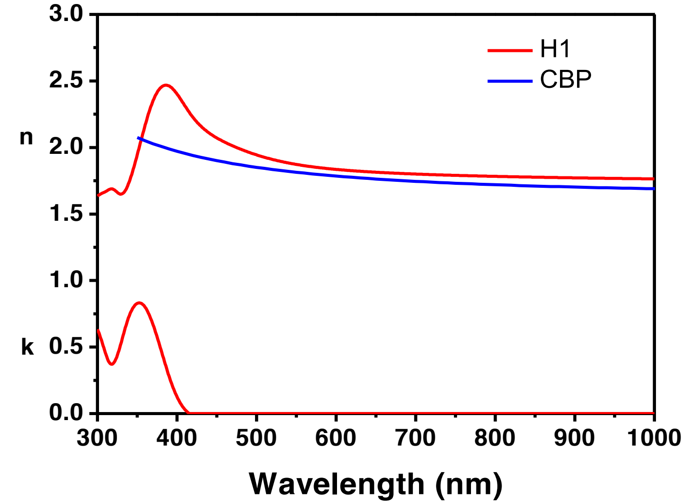


| Device | $J_{sc}$ [mA/cm$^2$] | $V_{oc}$ [V] | FF | PCE [%] | APT [%] | LUE [%] |
|---|---|---|---|---|---|---|
| WO OC | 18.4 | 0.72 | 0.62 | 8.3 | 30.2 | 2.51 |
| W OC-1 | 18.1 | 0.74 | 0.65 | 8.7 | 48.3 | 4.20 |
| W-OC-2 | - | - | - | - | 51.2 | 5.2 |

Li, et al. Adv. Mater., 31, 1903173 (2019)